ESC European Society of Cardiology

Cardiovascular Research (2019) **115**, 1952–1962
doi:10.1093/cvr/cvz162

INVITED REVIEW

Frontiers in positron emission tomography imaging of the vulnerable atherosclerotic plaque

Mark G. MacAskill [1,2]*, David E. Newby [1], and Adriana A.S. Tavares[1,2]

[1]University/BHF Centre for Cardiovascular Science, University of Edinburgh, Edinburgh, UK; and [2]Edinburgh Imaging, University of Edinburgh, Edinburgh, UK

Received 31 January 2019; revised 16 April 2019; editorial decision 15 May 2019; accepted 19 June 2019; online publish-ahead-of-print 24 June 2019

Abstract Rupture of vulnerable atherosclerotic plaques leading to an atherothrombotic event is the primary driver of myocardial infarction and stroke. The ability to detect non-invasively the presence and evolution of vulnerable plaques could have a huge impact on the future identification and management of atherosclerotic cardiovascular disease. Positron emission tomography (PET) imaging with an appropriate radiotracer has the potential to achieve this goal. This review will discuss the biological hallmarks of plaque vulnerability before going on to evaluate and to present PET imaging approaches which target these processes. The focus of this review will be on techniques beyond [^{18}F]FDG imaging, some of which are clinically advanced, and others which are on the horizon. As inflammation is the primary driving force behind atherosclerotic plaque development, we will predominantly focus on approaches which either directly, or indirectly, target this process.

Keywords Atherosclerosis • Vulnerable plaque • PET • Inflammation

1. Introduction

Cardiovascular disease is the number one cause of mortality globally, representing 31% of all deaths.[1] Of these deaths, 85% are due to myocardial infarction and stroke. Atherosclerotic plaque rupture is present in the majority of patients who have suffered a fatal myocardial infarction,[2] and plays a major role in the onset of stroke.[3] Therefore, a non-invasive imaging approach, which is capable of identifying vulnerable plaques is the ultimate goal for imaging in cardiovascular disease. It should be noted that molecular imaging is being developed for all forms of non-invasive imaging including single-photon emission computed tomography (SPECT), optical imaging, magnetic resonance imaging (MRI) and ultrasound, although this review will focus on those in development for positron emission tomography (PET) imaging only.

PET imaging is at the forefront of novel and non-invasive molecular imaging modalities as it is based on the use of selective radiotracers targeting specific biochemical processes *in vivo*.[4] The use of a radiotracer permits exceptional target specificity and sensitivity at the molecular level that cannot be accomplished with other imaging techniques[5]; allowing the cardiovascular field to move beyond structural or perfusion imaging into highly sensitive detection of molecular processes. However, a disadvantage of PET imaging is the limited spatial resolution and poor anatomic context compared with other techniques, such as computed tomography (CT) and MRI, which are less sensitive but have higher spatial resolution.[6] In this regard, hybrid imaging systems combining PET with CT or MRI have significant potential. PET/CT is the most widely used dual modality of the two, with CT providing anatomical data to complement PET with or without blood contrast agents. More importantly, CT is integral to attenuation correction of PET data, a major challenge which is the subject of much research in PET/MRI.[7] However, PET/MRI has excellent soft tissue contrast which is a major advantage for cardiovascular disease, in addition to potentially allowing the addition of various MRI sequences such as T1-weighted direct thrombus imaging. Notwithstanding, the justification of hybrid imaging system should be carefully considered based on the desired application, with a previous clinical study demonstrating that multimodal imaging does not always improve diagnostic accuracy.[8]

Despite the advantages associated with the use of PET for molecular imaging, other limitations in addition to low-spatial resolution must be considered. PET is associated with relatively high scanning costs and demanding scanning pipelines compared with other imaging modalities, such as SPECT, ultrasound, or CT, as it requires the production of a radiotracer prior to initiating patient scanning.[9] Access to selective radiotracers for clinical PET imaging has been a bottleneck to the wider clinical use of this technique. However, with the advent of PET radionuclide generators, as well as the development of simpler and high yield radiosynthesis methods, this bottleneck is likely to be overcome in the near future. The ionizing radiation associated with PET imaging has also stigmatized the widespread use of this imaging technique in the clinic, in spite of the fact that radiation exposure from a whole-body PET scan

* Corresponding author. Tel: 0131 242 6735; fax: 0131 242 6779, E-mail: mark.macaskill@ed.ac.uk

(c. 6 mSv) is similar to one chest CT (c. 10 mSv).[10] Therefore, there is a need for the education of researchers, clinicians, and the general public on the true risks of radiation while keeping patient benefit in mind. The established, accepted and routine use of [^{18}F]FDG in the clinical management of cancer patients is a clear example that clinical PET imaging is feasible. The soon-to-be commercially available total body PET scanner brings further hope for widespread use of clinical PET imaging, as the radiation dose can be reduced substantially while preserving a considerable gain in sensitivity.[11]

PET imaging holds particular potential as we travel through the era of personalized medicine. Oncology and neurology already use PET imaging extensively as a biomarker for diagnosis, staging and treatment monitoring.[12,13] Cardiology is the next field where PET imaging could thrive. Despite challenges with heart motion and small size of arterial and venous networks, current PET imaging test–retest results are typically around 15%.[14,15] The development of more selective radiotracers will resolve the issues around undesirable uptake in cardiac muscle. Moreover, standardization of multicentre PET imaging data is possible for cardiovascular or other applications, as proven by several historical and large quantitative brain PET studies (e.g. PPMI, NCT01141023, and ADNI, NCT00106899).

2. Atherosclerosis and plaque vulnerability

The development of an atherosclerotic plaque is a dynamic process which occurs throughout the adult lifespan, starting with intimal lesions in early adulthood through to complex atherosclerotic plaques later in life. These plaques occur within medium-large arteries and are the result of a non-resolving chronic inflammatory process which occurs at sites of blood flow disturbance.[16] Progression of plaque development is fuelled by the accumulation of low-density lipoprotein (LDL) cholesterol within the intima, leading to the infiltration of inflammatory cells which results in a negative cycle of remodelling.[17] Based on post-mortem histological studies, progressive atherosclerotic plaques can be grouped into several categories (*Table 1*).[18] These categories can describe both stable and vulnerable plaques, the latter of which are defined as an event prone plaque,[19] i.e. prone to rupture. Symptomatic stable plaques can usually be detected with angiography due to their luminal occlusive nature, although vulnerable plaques are not as readily detectible and often clinically silent prior to an event. Rupture of vulnerable thin fibrous cap atheroma is the leading cause of occlusive thrombus formation, and the identification of these plaques prior to an event is paramount.[19] Thickness of the fibrous cap is the best discriminator of plaque rupture, with a cap thickness less than 55 μm representing a critical threshold in a post-mortem histological study.[20] The following section of this review will highlight some of the biological fingerprints of the vulnerable plaque which also have potential as imaging targets as detailed later in the review.

3. Biological fingerprint of the vulnerable atherosclerotic plaque

The development and progression of atherosclerotic plaques is driven by a balance between pro-inflammatory and anti-inflammatory processes.[21] Macrophage accumulation within the plaque is a major component of atherosclerosis, although other immune cells, such as monocytes, dendritic cells, lymphocytes, eosinophils, and mast cells, also play an important role.[16,22] Intimal macrophages differentiate into foam cells following the scavenging of lipoprotein-derived cholesterol.[23] The presence of macrophages within the plaque is a significant risk factor for rupture.[20] In addition, the balance of polarization between M1 and M2 macrophages can have a major impact on atherosclerotic progression. A clinical post-mortem study demonstrated the presence of both subsets of macrophages within developing and vulnerable plaques. Within the latter, pro-inflammatory M1 macrophages dominated the rupture prone shoulder regions of the fibrous cap, while the remainder of the cap showed equal expression of M1 and anti-inflammatory M2 phenotypes.[24] This suggests that an imaging approach targeting M1 over M2 macrophages may provide some specificity towards vulnerable plaques. However, due to the plasticity of these phenotypes and the abundance of both within atherosclerotic lesions, this approach may be too restrictive. In addition, there is evidence to suggest that most foam cells express an M2 phenotype.[25] Therefore, imaging approaches targeting M1, M2, or pan-macrophage phenotypes all have potential and should be explored.

Inflammation is also a driver for a number of secondary hallmarks of plaque vulnerability. Intraplaque calcification is initiated by inflammation, and also thought to be part of a positive feedback mechanism which further propagates the cycle.[26,27]

Intra-plaque angiogenesis is another key feature of vulnerable atherosclerotic plaques, responsible for the development of unsupported leaky neovessels. This contributes to plaque instability through intra-plaque haemorrhage and inflammatory cell infiltration.[28] The abnormal presence of microvessels in the intima of atherosclerotic lesions relative to healthy vessel intima was reported as early as 1936.[29] However, in the last few decades, this vulnerability risk factor has come to the fore. While angiogenesis is through to play a role in early plaque development,[30] the presence of extensive intra-plaque neovessels in mature plaques is closely associated with vulnerability.[31] Intraplaque haemorrhage in humans is increased in vulnerable plaques compared to erosion and fibrocalcific lesions.[18] Additionally, total microvessel density is increased in ruptured plaques versus non-ruptured,[32] and in lesions with severe macrophage infiltration at the cap and the shoulders of the plaque. Furthermore, expansion of the perivascular network termed the vasa vasorum is also associated with plaque instability.[33,34] Therefore, the detection of plaque angiogenesis presents another target for clinical diagnosis of at risk lesions. An alternative strategy is to directly target the haemorrhage using activated platelet markers. Through the expansion of leaky neovessels, deposition of activated platelets within the plaque directly stimulates inflammatory cell extravasation, contributing to plaque progression.[35] This target could also be useful downstream of plaque rupture to target acute arterial thrombosis.

Upstream of angiogenesis, another feature of the vulnerable plaque is hypoxia. Intraplaque hypoxia is the result of an expanding plaque, particularly with large areas of necrosis.[31] The extent of hypoxia within symptomatic carotid plaques has been demonstrated in a clinical study using the hypoxia marker pimonidazole, which was infused into patients prior to carotid endarterectomy.[36] The level of hypoxia within the lesions correlated with thrombus and angiogenesis, as well as being increased when compared to early plaques. However, in this small clinical study, the level of hypoxia was also increased within stable plaques. Preclinically, the low-density lipoprotein receptor knockout (LDLR$^{-/-}$) atherosclerosis model has been used to demonstrate that hypoxia is causally related to necrotic core expansion within plaques.[37] It remains to be seen whether targeting plaque hypoxia is specific enough to detect plaque vulnerability.

Table 1 Modified American Heart Association (AHA) classification of atherosclerotic lesions based on description[18]

AHA classification based on morphological description		
Lesion type	**Descriptions**	**Thrombosis**
Non-atherosclerotic intimal lesions		
Intimal thickening	The normal accumulation of smooth muscle cells (SMCs) in the intima in the absence of lipid or macrophage foam cells.	Absent
Intimal xanthoma, or 'fatty streak'	Luminal accumulation of foam cells without a necrotic core or fibrous cap. Based on animal and human data, such lesions usually regress.	Absent
Progressive atherosclerotic lesions		
Pathological intimal thickening	SMCs in a proteoglycan-rich matrix with areas of extracellular lipid accumulation without necrosis.	Absent
With erosion	Luminal thrombosis; plaque same as above.	Thrombus mostly mural and infrequently occlusive
Fibrous cap atheroma	Well-formed necrotic core with an overlying fibrous cap.	Absent
With erosion	Luminal thrombosis; plaque same as above; no communication of thrombus with necrotic core.	Thrombus mostly mural and infrequently occlusive
Thin fibrous cap atheroma	A thin fibrous cap infiltrated by macrophages and lymphocytes with rare SMCs and an underlying necrotic core.	Absent; may contain intraplaque haemorrhage/fibrin
Plaque rupture	Fibroatheroma with cap disruption; luminal thrombus communicates with the underlying necrotic core.	Thrombus usually occlusive
Calcified nodule	Eruptive nodular calcification with underlying fibrocalcific plaque.	Thrombus usually non-occlusive
Fibrocalcific plaque	Collagen-rich plaque with significant stenosis usually contains large areas of calcification with few inflammatory cells; a necrotic core may be present.	Absent

However, this process clearly plays a major role in the progression of atherosclerosis and therefore should not be discounted at this stage.

Apoptosis, the programmed death of cells, is another potential imaging target in vulnerable plaques. Macrophages account for the majority of apoptotic cells within atherosclerotic plaques.[38] Preclinically, it has been proposed that apoptosis of macrophages in early lesion development is atheroprotective due to negative regulation of inflammation. Whereas, in more developed lesions, macrophage apoptosis is proposed to be proatherogenic due to the loss of these cells on the efferocytosis process.[39,40] Perhaps more straightforward is the negative impact of endothelial cell and vascular smooth muscle cell apoptosis, leading to increased incidences of plaque erosion[41] and destabilization of the plaque cap,[42] respectively.

As our understanding of atherosclerosis and plaque vulnerability develops, there is an even greater need to develop novel imaging approaches beyond those which are currently clinically available.[19] *Figure 1* summaries the imaging approaches and targets which are discussed within this review.

4. Inflammation

As atherosclerosis is the result of a non-resolving chronic inflammatory process,[16] the most common approach in vulnerable plaque imaging is naturally the direct or indirect targeting of inflammation.

4.1 Glucose metabolism

To date, PET imaging of inflammation has largely been carried out by targeting glucose metabolism using [^{18}F]FDG. This can serve as a non-specific surrogate for inflammation which relies on the highly metabolic state of vascular macrophages where [^{18}F]FDG competes with physiological glucose and becomes trapped within the cells.[43] There are several recently published reviews which excellently summarize the use of [^{18}F]FDG in atherosclerosis,[44–46] therefore, the main focus of this review will be on alternative PET imaging approaches which are at an earlier stage of investigation. The ability of [^{18}F]FDG to image atherosclerotic plaque uptake was first shown by Rudd *et al.*[47] in 2002, demonstrating a 30% increase in carotid artery uptake in symptomatic patients. In 500 patients devoid of a histology of cardiovascular disease, [^{18}F]FDG uptake in the ascending aorta was found to strongly predict the development of cardiovascular disease beyond the predictive ability of Framingham risk score.[48] Studies have also identified a [^{18}F]FDG uptake in macrophage-rich areas of human plaques,[47,49] supporting the hypothesis that [^{18}F]FDG uptake is largely due to macrophages.

[^{18}F]FDG PET imaging has several disadvantages which hold back the potential of this approach. Firstly, due to the non-specific nature of [^{18}F]FDG uptake, this radiotracer is taken up by other metabolizing cells. This is a particular issue when studying the coronary arteries where [^{18}F]FDG uptake in the myocardium makes vascular localization difficult, leading to the development of additional fasting protocols to improve this issue.[50] The indiscriminate nature of [^{18}F]FDG uptake also makes it difficult to identify the true source of [^{18}F]FDG uptake in plaques, which will inevitability compound the ability of this approach to distinguish between stable and vulnerable plaques.[51] Other than inflammation, [^{18}F]FDG uptake has been shown to closely correlate with other cellular events such as hypoxia.[52] Additionally, pre-scan hyperglycaemia has been shown to impact standardized uptake value outcome measures from [^{18}F]FDG scans.[53]

4.2 18 kDa translocator protein

After [^{18}F]FDG, the targeting of the 18 kDa translocator protein (TSPO) is one of the most widely utilized PET imaging approaches for

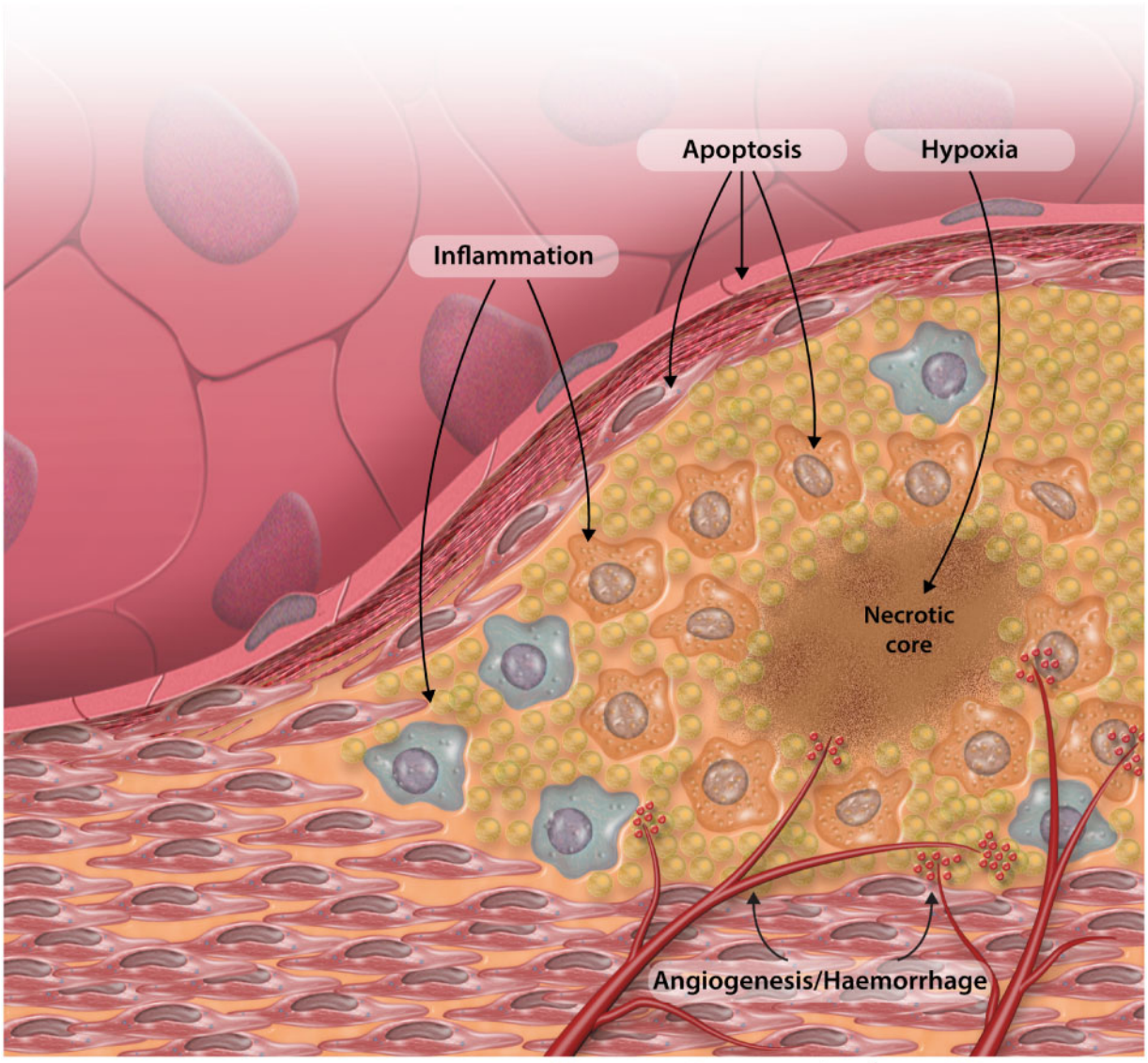

Inflammation

Glucose metabolism	[^{18}F]FDG		***CXCR4***	[^{68}Ga]oentixafor	
TSPO	[^{11}C]PK11195	[^{18}F]FEDAA1106	***SST2***	[^{68}Ga]DOTATATE	[^{68}Ga]DOTANOC
	[^{18}F]-FEMPA	[^{18}F]GE-180	***FR*β**	[^{18}F]-FOL	
Micro- calcification	[^{18}F]NaF		***COX***	[^{11}C]PS13	[^{11}C]MC1

Angiogenesis			Haemorrhage	Hypoxia	Apoptosis
α***V*β*3***	[^{18}F]Galacto-RGD	[^{18}F]Fluciclatide	[^{18}F]-GP1	[^{18}F]-FMISO	[^{18}F]ML-10
α***7nAChR***	[^{18}F]ASEM	[^{11}C]NS14492 [^{18}F]NS14490		[^{18}F]-HX4	

Figure 1 Schematic illustration of imaging targets, along with their relevant radiotracers, targeting the vulnerable atherosclerotic plaque.

inflammation. TSPO, formally termed the peripheral benzodiazepine receptor,[54] is found on the outer membrane of the mitochondria where it transports cholesterol for steroidogenesis.[55] While TSPO is present throughout the body, it is highly expressed in macrophages and can be used as a biomarker for localized inflammation.[56,57] Traditionally, TSPO imaging has been developed to detect neuroinflammation across a number of disorders by targeting activated microglia.[58,59] However, there are several preclinical and clinical studies investigating this approach in atherosclerosis utilizing radiotracers, such as [^{11}C]PK11195—the archetypical TSPO ligand developed several decades ago.[60] In a murine atherogenic model, [^{11}C]PK11195 uptake is increased in inflamed regions of the aorta.[61] However, uptake is also present within healthy aortas, with no difference in the overall binding compared with atherosclerotic aorta. This is likely due to the relatively high non-specific binding which has limited the use of [^{11}C]PK11195 in other areas.[62] Newly developed alternatives to [^{11}C]PK11195 include [^{18}F]FEDAA1106, which has been assessed using a constrictive cuff placed around the carotid artery of apolipoprotein E-deficient mice to induce atherosclerotic-like lesions.[63] [^{18}F]FEDAA1106 uptake was higher in the cuffed artery and was more consistent with inflamed regions compared with [^{18}F]FDG. Two other TSPO radiotracers have also been assessed in preclinical atherosclerotic models, [^{18}F]-FEMPA[64] and the more recent [^{18}F]GE-180.[65] Both have higher uptake in macrophage-rich areas but also failed to show increased uptake in in atherosclerotic compared with healthy vessels. A limited number of clinical studies have assessed [^{11}C]PK11195. First, using *ex vivo* human carotid endarterectomy specimens, [^{11}C]PK11195 uptake correlated with macrophage-rich regions,[57] similar to previous preclinical studies. Following this, another group was the first to demonstrate the ability of [^{11}C]PK11195 to identify culprit plaques in a small clinical study of symptomatic patients.[66] In this study, a sensitivity of 78% and specificity of 74% was reported for the identification of symptomatic patients with cerebrovascular events, providing a strong rationale to continue developing this imaging approach.

Over 80 radiotracers with high affinity for TSPO have been developed and assessed.[67] Despite this, there remains no widely accepted strategy to image this target, in part due to conflicting outcomes from various clinical trials. A seminal study published in 2012 revealed that a single human genetic polymorphism, rs6971, drastically changes the binding affinity of TSPO ligands across the population,[68] which might explain part of the conflicting outcomes of previously reported TSPO PET clinical studies. The difference between high binders and low binders can be as large as 50 times for ligands such as [^{11}C]PBR28.[69] Interestingly, the only TSPO ligand which is not effected by the genetic polymorphism is [^{11}C]PK11195.[68] Efforts within the TSPO radiotracer development field are now shifting towards the discovery of a ligand which is insensitive to the polymorphism, or is usable in low-affinity binders, and has improved characteristics compared with [^{11}C]PK11195. To date, one of the most promising ligands is [^{11}C]ER176 which is based on the structure of [^{11}C]PK11195 and has a low to high binding ratio of 3.[70]

4.3 Microcalcification

The formation of calcium within plaques is thought to be driven by inflammation leading to an actively regulated pathophysiologic process, much like the formation of bone.[26,71] Key proinflammatory cytokines derived from macrophages, such as interleukin-6 and tumour necrosis factor-α, increase vascular smooth muscle cell calcification in a paracrine manner.[27] Intraplaque calcification can be split into two different terms depending on the size of the deposit. Macrocalcification describes the largest deposits within a plaque, considered to be larger than 50 μm, with deposits smaller than 50 μm termed microcalcification.[27] In aortic stenosis, microcalcified deposits lead onto the development of macrocalcification,[72] which in atherosclerosis confers mechanical plaque stability while microcalcification is considered a feature of plaque vulnerability.[73] Macrocalcification can be readily detected by CT, with coronary artery calcium scoring (CAC), and progression of CAC, already used as surrogate markers of atherosclerotic burden and cardiovascular risk.[74,75] The only non-invasive imaging approach able to reliably detect microcalcification is PET imaging with [^{18}F]NaF, which is incorporated into deposits by exchanging the hydroxyl ions of hydroxyapatite crystals with radiolabelled fluoride to form fluorapatite.[76,77] Additionally, [^{18}F]NaF may also be able to detect areas of tissue necrosis as demonstrated in the infarcted heart,[78,79] as well as correlating with peri-coronary adipose tissue density which is another marker of vascular inflammation.[80]

As [^{18}F]NaF has long been available in humans for other conditions, the majority of studies investigating [^{18}F]NaF imaging have been clinical. One of the first studies to demonstrate the feasibility of this approach was carried out in 2010 using a retrospective dataset of 75 whole-body PET scans to demonstrate the colocalization of mineral deposition with arterial wall alterations.[81] In a follow-up study in 269 oncologic patients [^{18}F]NaF accumulation in the common carotid arteries was investigated,[82] with 34.9% of patients showing carotid [^{18}F]NaF uptake which colocalized with CT measured calcification. Radiotracer uptake was associated with multiple cardiovascular risk factors including hypertension and hypercholesterolaemia. One of the first prospective studies to investigate [^{18}F]NaF uptake in coronary arteries demonstrated a higher uptake of radiotracer in patients with coronary atherosclerosis, and more importantly, high [^{18}F]NaF uptake was associated with a higher rate of previous cardiovascular events.[83] Additionally, [^{18}F]NaF uptake in patients with myocardial infarction and stable angina have a higher [^{18}F]NaF uptake in culprit compared with non-culprit plaques, with marked uptake at all carotid plaque ruptures.[84] Stable angina patients with focal radiotracer uptake were associated with more high-risk features on intravascular ultrasound. A seminal clinical study, the PRE^{18}FFIR trial, is currently underway to determine the predictive potential of [^{18}F]NaF to predict recurring clinical events by identifying high-risk coronary plaques (Clinical Trials No. NCT02278211).

With strong evidence for the use of [^{18}F]NaF in intraplaque microcalcification, a better understanding of the precise molecular mechanism of vascular uptake is needed. Using a number of techniques, including micro PET/CT, autoradiography and histology, carotid endarterectomy specimens have been utilized to determine the nature of [^{18}F]NaF uptake.[73] The outcome of this study demonstrated that [^{18}F]NaF was highly selective for areas of microcalcification over macrocalcification which, the authors speculate, is due to the increased surface area within microcalcified deposits. [^{18}F]NaF binding in a swine coronary artery disease model has demonstrated the presence of microcalcification in early neointimal lesions before the development of clinically significant lesions identified by other modalities.[85] This imaging approach is perhaps the most promising and clinically advanced of the options discussed within this review. Moving forward, this target would greatly benefit from further preclinical studies using models of atherosclerosis in order to understand the relation of microcalcification to the pathophysiology of atherosclerosis.

4.4 Chemokine receptor 4

Chemokines are a family of small molecules which exert chemotactic effects on cells. CXC chemokine receptor 4 (CXCR4) is the receptor for CXC Chemokine Ligand 12 (CXCL12) and is expressed on endothelial and smooth muscle cells; as well as inflammatory cells such as

monocytes, macrophages, and leucocytes.[86] The exact role of CXCL12/CXCR4 in atherosclerosis is not yet known, although several studies report different functions dependent on cell type. CXCR4 expression in smooth muscle cells may be beneficial in atherosclerosis as administration of CXCL12 in atherosclerotic mice results in a thicker fibrous cap due to cell recruitment.[87] In endothelial cells, CXCR4 may also play a positive role by stimulating the recruitment of endothelial progenitor cells to the plaque.[88] Conversely, CXCR4 stimulation in macrophages can lead to increased pinocytosis which may cause the accumulation of oxidized LDL and therefore the formation of foam cells.[86,88] Due to the role of CXCR4 in the atherogenic process, interest in targeting this receptor has increase over recent years with the advent of the highly selective radiotracer [^{68}Ga]pentixafor. Several studies have investigated this approach in preclinical and clinical settings. In a rabbit atherosclerosis model, [^{68}Ga]pentixafor uptake was increased in injured atherosclerotic vessels compared with healthy controls.[89] Additionally, autoradiography experiments demonstrated [^{125}I]pentixafor uptake was located in macrophage-rich regions within the plaques. One of the first clinical studies to investigate arterial binding and clinical correlates of [^{68}Ga]pentixafor uptake was carried out retrospectively in 51 patients who were scanned for non-cardiovascular indications.[90] Focal arterial radiotracer uptake was seen in all individuals, with the levels of uptake correlating with calcified plaque burden and cardiovascular risk factors. In the same year, a similar retrospective clinical study was carried out in 38 patients, 34 of which showed arterial uptake of [^{68}Ga]pentixafor.[91] High levels of [^{68}Ga]pentixafor uptake correlated with cardiovascular risk factors. [^{68}Ga]pentixafor uptake in plaques of patients who have recently suffered a myocardial infarction is higher in culprit lesions.[92] The same study used *ex vivo* cadaveric coronary artery specimens demonstrating [^{68}Ga]pentixafor mainly colocalized with CD68^{+} inflammatory cells.

4.5 Somatostatin receptor subtype 2

The somatostatin receptor subtype 2 (SST2) is a G-protein-coupled receptor which is through to play a role in mediation of the immune system via the nervous system through the release of immumopeptides.[93] Expression of SST2 is highly up-regulated in macrophages which are challenged by an inflammatory stimulus such as lipopolysaccharides.[94] The SST2 selective radiotracer [^{68}Ga]DOTATATE was developed in 2002 in order to identify SST2 expressing tumours,[95] and more recently has undergone investigation in atherosclerosis. Using a murine atherosclerosis model, *ex vivo* autoradiography revealed radiotracer uptake in aortic plaques which correlated with macrophage-rich regions.[96] A similar finding was found in a later preclinical study also using mice where it was also noted that the alternative SST2 radiotracer [^{68}Ga]DOTANOC had a higher aorta-to-blood ratio than [^{68}Ga]DOTATATE.[97] In a retrospective clinical study of 70 oncology patients [^{68}Ga]DOTATATE PET uptake was detected in all subjects and correlated with the presence of calcified plaques and prior vascular events.[98] More recently, in a prospective clinical study of 20 patients who had recently suffered a carotid event no difference was demonstrated between uptake in symptomatic compared with contralateral asymptomatic plaques.[99] This was due to a lack of SST2 expression demonstrated in follow up endarterectomy specimens. [^{68}Ga]DOTATATE uptake in 24 unstable patients who had recently experienced a clinical event successfully identified culprit plaques in the coronary and carotid arteries.[100] A mean of maximum tissue-to-blood ratio >2.66 identified culprit segments with a sensitivity of 87.5% and a specificity of 78.4%. In addition, [^{68}Ga]DOTATATE out performed [^{18}F]FDG in the coronaries where myocardial uptake of [^{18}F]FDG rendered scans uninterpretable. These studies highlight the potential for targeting SST2 in vulnerable plaques and warrant further large scale clinical trials.

4.6 Folate receptor-β

The folate receptor-β (FRβ) is a glycoprotein which is expressed on the surface of activated macrophages, but importantly is absent from resting macrophages and other inflammatory cells.[101] Endogenously this receptor mediates the delivery of folic acid and its derivatives into the interior of a small subset of cells within the body, thus making it an attractive target for therapeutic delivery in addition to imaging.[102] To date, folate imaging has largely been carried out in cancer and rheumatoid arthritis, although several studies have investigated this approach in atherosclerosis. Preclinical imaging in a murine atherosclerosis model using a SPECT folate radiotracer termed [^{99m}Tc]EC20 results in increased uptake of the agent in the plaques of mice on a western diet.[103] Following depletion of macrophages and monocytes with clodronate liposome treatment uptake of [^{99m}Tc]EC20 within plaques is significantly reduced, demonstrating the macrophage-specific uptake of this approach. Using a another folate SPECT agent [^{99m}Tc]-folate, high levels of radiotracer accumulate in areas rich in M2-like macrophages within carotid endarterectomy specimens.[104] More recently, a study utilized atherosclerotic plaques from mice, rabbits and humans to investigate the potential of the PET agent [^{18}F]FOL relative to [^{18}F]FDG.[105] [^{18}F]FOL colocalized with FRβ positive macrophages within carotid endarterectomy specimens from patients who recently suffered an ischaemic event. In the atherosclerotic mouse model [^{18}F]FOL binding was significantly higher versus healthy controls and correlated with macrophage density. In both mouse and rabbit models [^{18}F]FOL had a target to background ratio as high as [^{18}F]FDG, without the issue of high myocardial uptake.

4.7 Cyclooxygenase 1/2

Cyclooxygenase (COX) is the rate-limiting enzyme which converts arachidonic acid into prostanoids in order to mediate an inflammatory response. There are two forms of COX, COX-1 is the constitutively active from of the enzyme responsible for homeostasis, while COX-2 is the inducible form associated with proinflammatory responses.[106] Currently, COX imaging has yet to be explored in the field of atherosclerosis; however, radiotracers for these targets are currently being developed.[106] For example, [^{11}C]PS13 targets COX-1 and has widespread uptake in healthy rhesus monkeys. [^{11}C]MC1 targets COX-2, and in the same study, had no uptake within healthy subjects, in agreement with the inducible nature of COX-2. COX-2 has been shown to play a role in atherosclerosis by catalysing the production of Prostaglandin E2 which causes up-regulation of matrix metalloproteinases leading to plaque destabilization.[106] Whether this approach is selective enough to be used to detect vulnerable atherosclerotic plaques is yet to be shown.

4.8 Selectivity of inflammation imaging targets for atherosclerosis

As discussed above, there is a wide array of imaging approaches under development for detection of inflammation within atherosclerotic plaques. However, comparison studies are needed to clarify the following points: (i) what cell type, phenotype or process does each approach target, and (ii) which approach is better at assessing plaque vulnerability? A common experimental design so far has been to undertake comparison studies relative to [^{18}F]FDG. Recently, a study using human leukocyte subpopulations and polarized macrophages was conducted to determine the suitability and specificity of a number of radiotracers.[107,108] Of these,

[^{18}F]FDG had the highest uptake in macrophages, followed by a TSPO targeted radiotracer ([^{18}F]GE-180). [^{18}F]FDG and [^{18}F]GE-180 uptake was higher in M1 macrophages and monocytes versus other leukocyte subpopulations, contrasting with the CXCR4 targeting ([^{68}Ga]pentixafor) which did not distinguish between M1/M2 or leukocyte subpopulations. As improved radiotracers become available more complex comparison studies, preclinical and clinical, are necessary.

5. Angiogenesis

There is a large overlap in expression of angiogenic biomarkers in endothelial and inflammatory cells, e.g. CD31.[109] Furthermore, a number of non-endothelial cell types, such as macrophages,[110] play a major role in the angiogenic response. Therefore, imaging biomarkers which target specific molecular pathways of the angiogenic process, rather than cell type-specific targets, can be advantageous to non-invasively assess vulnerable plaques.

5.1 αVβ3 integrin

αVβ3 is an integrin which is closely associated with sprouting endothelial cells and is essential during angiogenesis.[111,112] This integrin is also highly expressed by macrophages and may play an important role in foam cell formation.[113] There are a number of radiotracers based on the RGD peptide targeting αVβ3 integrin. [^{18}F]Galacto-RGD was among one of the first RGD radiotracers to be explored in atherosclerosis.[114] In an atherosclerotic mouse model, [^{18}F]Galacto-RGD uptake was increased within the aorta relative to control C57Bl/6N mice. However, as is the case with many murine atherosclerosis models, no intraplaque angiogenesis was present and therefore following *ex vivo* investigation the signal was attributed to macrophage uptake. [^{18}F]Galacto-RGD has also been investigated in a small number (10) of human carotid arteries which had a high-grade stenosis relative to contralateral arteries.[115] Radiotracer target to background ratios were significantly higher in stenotic compared with non-stenotic areas, which correlated with αVβ3 integrin expression but failed to correlate with macrophage or microvessel density. While this study highlights the potential of [^{18}F]Galacto-RGD in atherosclerosis, the use of stenotic vessels which were not particularly vulnerable limits the conclusions which can be drawn in terms of suitability for identification of vulnerability.

Another αVβ3 integrin radiotracer, [^{18}F]Fluciclatide, has largely been developed in an oncology setting where it has been used clinically to assess tumour angiogenesis in response to therapeutic interventions.[116] Recently, [^{18}F]-Fluciclatide has been used to demonstrate that its uptake within the aorta is a highly reproducible marker of atherosclerotic burden in 46 subjects with a mixture of ischaemic heart disease, aortic stenosis, and healthy controls.[117] It should be noted that this imaging approach may also bind to areas of fibrosis, as demonstrated in the lungs, which may account for some of the uptake within plaques.[118] Targeting inflammation and angiogenesis in atherosclerosis when using this approach may prove to be a major advantage if further studies are performed in more suitable preclinical models and vulnerable human cohorts.

5.2 α7 Nicotinic acetylcholine receptor

The α7 nicotinic acetylcholine receptor (α7nAChR) is one subtype of a number of nicotinic receptors, consisting of a pentameric ligand-gated cation channel. α7nAChR expression is widely associated with both central and peripheral neuronal cells[119] but is also expressed in non-neuronal cells such as epithelial, endothelial, and immune cells.[120] The focus of this section is on α7nAChR, as opposed to the other subtypes, as this is the mostly highly expressed on endothelial cells and plays an essential role in angiogenesis.[121] As is the case with αvβ3 integrin, α7nAChR is also expressed within macrophages. This serves to promote the survival of the pro-angiogenic M2 phenotype.[122] Conversely, α7nAChR activation increases LDL cholesterol uptake within macrophages, potentially contributing to the formation of foam cells.[123] Directly, the role of α7nAChR in atherosclerosis has been demonstrated in multiple preclinical studies through pharmacological and genetic manipulation. The α7nAChR partial agonist varenicline aggravated aortic atherosclerotic plaque development in atherosclerotic mice, which was blocked by the α7nAChR antagonist methyllycaconitine.[124] Additionally, atherosclerotic mice which received a bone marrow transplant from α7nAChR$^{-/-}$ mice have increased systemic inflammatory status and platelet function; however, no differences in plaque formation are evident.[125] To date, no studies have manipulated α7nAChR in atherosclerotic models which have intraplaque angiogenesis.

Overall, the evidence for the use of α7nAChR as an imaging target to investigate the vulnerable plaque is convincing, and there are a number of radiotracers currently under development as recently described in a detailed review.[126] As of yet, none of these radiotracers have been assessed in atherosclerosis. [^{18}F]ASEM is an example of an α7nAChR antagonist based radiotracer which has suitable properties for imaging the human brain.[127,128] Since there is no evidence to suggest whether an agonist or antagonist based approach is most suitable in atherosclerosis, alternative agonist-based radiotracers such as [^{11}C]NS14492[129] and [^{18}F]NS14490[130] should also be considered. [^{18}F]NS14490 selectively targets α7nAChR in mice, as well as having high metabolic stability.[130] Interestingly, [^{18}F]NS14490 also displays high uptake within vascular structures of the healthy pig brain, eluding to its potential for cardiovascular imaging.[131]

6. Intraplaque haemorrhage

One of the most promising targets for intraplaque haemorrhage is glycoprotein (GP) IIb/IIIa complex, a receptor which is expressed on the surface of activated platelets and is essential for platelet aggregation.[132] Histologically, GP IIb/IIIa is upregulated in unstable angina pectoris patients,[133] and is the target of novel ultrasound imaging agents targeting high-risk plaques in murine atherosclerosis.[134] GP IIb/IIIa can be targeted in PET imaging using [^{18}F]GP1, a recently developed radiotracer which has high affinity for this target.[135] [^{18}F]GP1 has also been through a phase 1 clinical trial, demonstrating that it could identify acute arterial thrombus across a number of cardiovascular pathologies, in addition to being safe for use with a favourable biodistribution/kinetic profile.[135] With further preclinical and clinical investigation, [^{18}F]GP1 could have significant potential.

7. Hypoxia and apoptosis

While hypoxia and apoptosis are distinct processes, they are also strongly interlinked in atherosclerosis through hypoxia-induced release of HIF-1α leading to stimulation of apoptosis.[136] [^{18}F]FMISO is a radiotracer which becomes reduced and trapped within hypoxic cells.[137] In a rabbit atherosclerosis model, aortic [^{18}F]FMISO uptake increased with time on atherosclerotic diet and was 2.5 times higher than non-atherosclerotic controls.[137] Hypoxia was histologically confirmed and shown to localize in macrophage-rich areas. Clinically, one of the first

studies to investigate [^{18}F]FMISO in atherosclerosis demonstrated increase uptake in symptomatic carotid plaques relative to asymptomatic.[52] A similar pattern was observed with [^{18}F]FDG suggesting that hypoxia is responsible for a significant component of FDG signal within plaques. More recently the radiotracer [^{18}F]HX4 was developed which has a similar uptake mechanism as [^{18}F]FMISO, but with an improved metabolic profile.[137] [^{18}F]HX4 was used to demonstrate a correlation between hypoxia and plaque burden in eight patients with a history of cardiovascular events, where the maximum radiotracer to background ratio was higher in plaque segments.[138]

The radiotracer [^{18}F]ML-10 binds to cell membranes within apoptotic cells in a manner similar to the apoptosis probe annexin V.[139] [^{18}F]ML-10 has been successfully used to detect apoptosis in a rabbit model of atherosclerosis, with localization of the radiotracer and apoptotic cell membranes confirmed by *ex vivo* histology and autoradiography.[140] The specificity of this approach for vulnerable atherosclerotic plaques has yet to be explored.

8. Concluding remarks

There are a number of potential molecular imaging targets and approaches which remain relatively unexplored in atherosclerosis. Even further potential could be unlocked through the complementary use of multiple radiotracers. Inflammation and calcification have been clinically assessed in atherosclerosis using a dual radiotracer approach,[141] a strategy which has also been utilized in tumour imaging.[142] The use of more advanced preclinical models, as well as a careful targeted clinical approach has great potential to identify an imaging approach which can have a major clinical impact in the treatment of atherosclerosis. So far, a vulnerable plaque targeted approach with the currently available diagnostic tools has yet to be realized.[143] The merits of this approach have been discussed extensively in recent reviews,[143,144] and should continue to be further investigated; particularly as more imaging approaches become available. Should the field shift towards a pan-vascular tree approach to diagnose at risk patients,[145] the same imaging options developed to target individual vulnerable plaques will be applicable and key to the success of this alterative strategy. Overall, it is the authors opinion that [^{18}F]NaF imaging holds the most promise for the immediate future in PET imaging of vulnerable atherosclerotic plaques. Over the longer term, more specific approaches targeting inflammation, perhaps via TSPO, and intraplaque angiogenesis/haemorrhage are most likely to be successful in the identification of high-risk patients.

Conflict of interest: none declared.

Funding

M.G.M. is funded by the British Heart Foundation (PG/17/83/33370). D.E.N. is funded by the British Heart Foundation (CH/09/002, RE/18/5/34216, RG/16/10/32375), and a Wellcome Trust Senior Investigator Award (WT103782AIA). A.A.S.T. is funded by the British Heart Foundation (RG/16/10/32375 and IRF reference 34354, CRM 0024777).

References

1. World Health Organization. Cardiovascular diseases (CVDs) Fact Sheet. 2017. https://www.who.int/news-room/fact-sheets/detail/cardiovascular-diseases-(cvds) (6 December 2018, date last accessed).
2. Falk E, Nakano M, Bentzon JF, Finn AV, Virmani R. Update on acute coronary syndromes: the pathologists' view. *Eur Heart J* 2013;**34**:719–728.
3. Kronzon I, Tunick PA. Aortic atherosclerotic disease and stroke. *Circulation* 2006;**114**:63–75.
4. Salvadori P. Radiopharmaceuticals, drug development and pharmaceutical regulations in Europe. *Curr Radiopharm* 2008;**1**:7–11.
5. Ruth TJ. The uses of radiotracers in the life sciences. *Reports Prog Phys* 2009;**72**:016701.
6. Kherlopian AR, Song T, Duan Q, Neimark MA, Po MJ, Gohagan JK, Laine AF. A review of imaging techniques for systems biology. *BMC Syst Biol* 2008;**2**:74–18.
7. Chen Y, An H. Attenuation correction of PET/MR imaging. *Magn Reson Imaging Clin N Am* 2017;**25**:245–255.
8. Danad I, Raijmakers PG, Driessen RS, Leipsic J, Raju R, Naoum C, Knuuti J, Mäki M, Underwood RS, Min JK, Elmore K, Stuijfzand WJ, van Royen N, Tulevski II, Somsen AG, Huisman MC, van Lingen AA, Heymans MW, van de Ven PM, van Kuijk C, Lammertsma AA, van Rossum AC, Knaapen P. Comparison of coronary CT angiography, SPECT, PET, and hybrid imaging for diagnosis of ischemic heart disease determined by fractional flow reserve. *JAMA Cardiol* 2017;**2**:1100–1107.
9. Schulthess GV, Burger C. Integrating imaging modalities: what makes sense from a workflow perspective? *Eur J Nucl Med Mol Imaging* 2010;**37**:980–990.
10. International Atomic Energy Agency Vienna (Austria) D of PI. Radiation, people and the environment. International Atomic Energy Agency (IAEA); 2004.
11. Cherry SR, Jones T, Karp JS, Qi J, Moses WW, Badawi RD. Total-body PET: maximizing sensitivity to create new opportunities for clinical research and patient care. *J Nucl Med* 2018;**59**:3–12.
12. Rohren EM, Turkington TG, Coleman RE. Clinical applications of PET in oncology. *Radiology* 2004;**231**:305–332.
13. Valotassiou V, Malamitsi J, Papatriantafyllou J, Dardiotis E, Tsougos I, Psimadas D, Alexiou S, Hadjigeorgiou G, Georgoulias P. SPECT and PET imaging in Alzheimer's disease. *Ann Nucl Med* 2018;**32**:583–593.
14. Croteau E, Renaud JM, McDonald M, Klein R, DaSilva JN, Beanlands RSB, DeKemp RA. Test-retest repeatability of myocardial blood flow and infarct size using ^{11}C-acetate micro-PET imaging in mice. *Eur J Nucl Med Mol Imaging* 2015;**42**:1589–1600.
15. Thackeray JT, Renaud JM, Kordos M, Klein R, Dekemp RA, Beanlands RSB, DaSilva JN. Test-retest repeatability of quantitative cardiac ^{11}C-meta-hydroxyephedrine measurements in rats by small animal positron emission tomography. *Nucl Med Biol* 2013;**40**:676–681.
16. Hansson GK, Libby P, Tabas I. Inflammation and plaque vulnerability. *J Intern Med* 2015;**278**:483–493.
17. Shah PK. Pathogenesis of atherosclerosis. *Essent Cardiol Princ Pract* 2013;**47**:377–386.
18. Virmani R, Kolodgie FD, Burke AP, Farb A, Schwartz SM. Lessons from sudden coronary death: a comprehensive morphological classification scheme for atherosclerotic lesions. *Arterioscler Thromb Vasc Biol* 2000;**20**:1262–1275.
19. Bourantas CV, Garcia-Garcia HM, Farooq V, Maehara A, Xu K, Généreux P, Diletti R, Muramatsu T, Fahy M, Weisz G, Stone GW, Serruys PW. Clinical and angiographic characteristics of patients likely to have vulnerable plaques: analysis from the PROSPECT study. *JACC Cardiovasc Imaging* 2013;**6**:1263–1272.
20. Narula J, Nakano M, Virmani R, Kolodgie FD, Petersen R, Newcomb R, Malik S, Fuster V, Finn AV. Histopathologic characteristics of atherosclerotic coronary disease and implications of the findings for the invasive and noninvasive detection of vulnerable plaques. *J Am Coll Cardiol* 2013;**61**:1041–1051.
21. Libby P, Tabas I, Fredman G, Fisher EA. Inflammation and its resolution as determinants of acute coronary syndromes. *Circ Res* 2014;**114**:1867–1879.
22. Moore KJ, Sheedy FJ, Fisher EA. Macrophages in atherosclerosis: a dynamic balance. *Nat Rev Immunol* 2013;**13**:709–721.
23. Chistiakov DA, Melnichenko AA, Myasoedova VA, Grechko AV, Orekhov AN. Mechanisms of foam cell formation in atherosclerosis. *J Mol Med Journal Med* 2017;**95**:1153–1165.
24. Stöger JL, Gijbels MJ, van der Velden S, Manca M, van der Loos CM, Biessen EA, Daemen MJ, Lutgens E, de Winther MP. Distribution of macrophage polarization markers in human atherosclerosis. *Atherosclerosis* 2012;**225**:461–468.
25. Oh J, Riek AE, Weng S, Petty M, Kim D, Colonna M, Cella M, Bernal-Mizrachi C. Endoplasmic reticulum stress controls M2 macrophage differentiation and foam cell formation. *J Biol Chem* 2012;**287**:11629–11641.
26. Chen W, Dilsizian V. Targeted PET/CT imaging of vulnerable atherosclerotic plaques: microcalcification with sodium fluoride and inflammation with fluorodeoxyglucose. *Curr Cardiol Rep* 2013;**15**:364.
27. Deuell KA, Callegari A, Giachelli CM, Rosenfeld ME, Scatena M. RANKL enhances macrophage paracrine pro-calcific activity in high phosphate-treated smooth muscle cells: dependence on IL-6 and TNF-α. *J Vasc Res* 2012;**49**:510–521.
28. Virmani R, Kolodgie FD, Burke AP, Finn AV, Gold HK, Tulenko TN, Wrenn SP, Narula J. Atherosclerotic plaque progression and vulnerability to rupture: angiogenesis as a source of intraplaque hemorrhage. *Arterioscler Thromb Vasc Biol* 2005;**25**:2054–2061.
29. Paterson J. Vascularization and hemorrhage of the intima of arteriosclerotic coronary arteries. *Arch Path* 1936;**22**:313–324.
30. Jeziorska M, Woolley DE. Neovascularization in early atherosclerotic lesions of human carotid arteries: its potential contribution to plaque development. *Hum Pathol* 1999;**30**:919–925.
31. Sluimer JC, Daemen MJ. Novel concepts in atherogenesis: angiogenesis and hypoxia in atherosclerosis. *J Pathol* 2009;**218**:7–29.

32. Moreno PR, Purushothaman KR, Fuster V, Echeverri D, Truszczynska H, Sharma SK, Badimon JJ, O'Connor WN. Plaque neovascularization is increased in ruptured atherosclerotic lesions of human aorta: implications for plaque vulnerability. *Circulation* 2004;**110**:2032–2038.
33. Sedding DG, Boyle EC, Demandt JAF, Sluimer JC, Dutzmann J, Haverich A, Bauersachs J. Vasa vasorum angiogenesis: key player in the initiation and progression of atherosclerosis and potential target for the treatment of cardiovascular disease. *Front Immunol* 2018;**9**:706.
34. Kolodgie FD, Virmani R, Burke AP, Farb A, Weber DK, Kutys R, Finn AV, Gold HK. Pathologic assessment of the vulnerable human coronary plaque. *Heart* 2004;**90**: 1385–1391.
35. Kral JB, Schrottmaier WC, Salzmann M, Assinger A. Platelet interaction with innate immune cells. *Transfus Med Hemother* 2016;**43**:78–88.
36. Sluimer JC, Gasc JM, van Wanroij JL, Kisters N, Groeneweg M, Sollewijn Gelpke MD, Cleutjens JP, van den Akker LH, Corvol P, Wouters BG, Daemen MJ, Bijnens A. Hypoxia, hypoxia-inducible transcription factor, and macrophages in human atherosclerotic plaques are correlated with intraplaque angiogenesis. *J Am Coll Cardiol* 2008;**51**:1258–1265.
37. Marsch E, Theelen TL, Demandt JA, Jeurissen M, van Gink M, Verjans R, Janssen A, Cleutjens JP, Meex SJ, Donners MM, Haenen GR, Schalkwijk CG, Dubois LJ, Lambin P, Mallat Z, Gijbels MJ, Heemskerk JW, Fisher EA, Biessen EA, Janssen BJ, Daemen MJ, Sluimer JC. Reversal of hypoxia in murine atherosclerosis prevents necrotic core expansion by enhancing efferocytosis. *Arterioscler Thromb Vasc Biol* 2014;**34**: 2545–2553.
38. Kolodgie FD, Narula J, Burke AP, Haider N, Farb A, Hui-Liang Y, Smialek J, Virmani R. Localization of apoptotic macrophages at the site of plaque rupture in sudden coronary death. *Am J Pathol* 2000;**157**:1259–1268.
39. Gautier EL, Huby T, Witztum JL, Ouzilleau B, Miller ER, Saint-Charles F, Aucouturier P, Chapman MJ, Lesnik P. Macrophage apoptosis exerts divergent effects on atherogenesis as a function of lesion stage. *Circulation* 2009;**119**: 1795–1804.
40. Van Vré EA, Ait-Oufella H, Tedgui A, Mallat Z. Apoptotic cell death and efferocytosis in atherosclerosis. *Arterioscler Thromb Vasc Biol* 2012;**32**:887–893.
41. White SJ, Newby AC, Johnson TW. Endothelial erosion of plaques as a substrate for coronary thrombosis. *Thromb Haemost* 2016;**115**:509–519.
42. Clarke MCH, Figg N, Maguire JJ, Davenport AP, Goddard M, Littlewood TD, Bennett MR. Apoptosis of vascular smooth muscle cells induces features of plaque vulnerability in atherosclerosis. *Nat Med* 2006;**12**:1075–1080.
43. Gallagher BM, Fowler JS, Gutterson NI, Macgregor RR, Wolf AP. Metabolic trapping as a principle of radiopharmaceuticals design: some factors responsible for the biodistribution of FDG. *J Nucl Med* 1978;**19**:1154–1161.
44. Tarkin JM, Joshi FR, Rudd J. PET imaging of inflammation in atherosclerosis. *Nat Rev Cardiol* 2014;**11**:443.
45. Moss AJ, Adamson PD, Newby DE, Dweck MR. Positron emission tomography imaging of coronary atherosclerosis. *Future Cardiol* 2016;**12**:483–496.
46. Andrews JPM, Fayad ZA, Dweck MR. New methods to image unstable atherosclerotic plaques. *Atherosclerosis* 2018;**272**:118–128.
47. Rudd JHF, Warburton EA, Fryer TD, Jones HA, Clark JC, Antoun N, JohnströM P, Davenport AP, Kirkpatrick PJ, Arch BN, Pickard JD, Weissberg PL. Imaging atherosclerotic plaque inflammation with [^{18}F]-fluorodeoxyglucose positron emission tomography. *Circulation* 2002;**105**:2708–2711.
48. Figueroa AL, Abdelbaky A, Truong QA, Corsini E, MacNabb MH, Lavender ZR, Lawler MA, Grinspoon SK, Brady TJ, Nasir K, Hoffmann U, Tawakol A. Measurement of arterial activity on routine FDG PET/CT images improves prediction of risk of future CV events. *JACC Cardiovasc Imaging* 2013;**6**:1250–1259.
49. Tawakol A, Migrino RQ, Bashian GG, Bedri S, Vermylen D, Cury RC, Yates D, LaMuraglia GM, Furie K, Houser S, Gewirtz H, Muller JE, Brady TJ, Fischman AJ. *In vivo* ^{18}F-fluorodeoxyglucose positron emission tomography imaging provides a noninvasive measure of carotid plaque inflammation in patients. *J Am Coll Cardiol* 2006; **48**:1818–1824.
50. DiCarli MF, Taqueti VR, Dorbala S, Osborne MT, Murthy VL, Hulten EA, Blankstein R, Skali H. Patient preparation for cardiac fluorine-18 fluorodeoxyglucose positron emission tomography imaging of inflammation. *J Nucl Cardiol* 2016;**24**:86–99.
51. Dilsizian V, Jadvar H. Science to practice: does FDG differentiate morphologically unstable from stable atherosclerotic plaque? *Radiology* 2017;**283**:1–3.
52. Joshi FR, Manavaki R, Fryer TD, Figg NL, Sluimer JC, Aigbirhio FI, Davenport AP, Kirkpatrick PJ, Warburton EA, Rudd J. Vascular imaging with ^{18}F-fluorodeoxyglucose positron emission tomography is influenced by hypoxia. *J Am Coll Cardiol* 2017;**69**: 1873–1874.
53. Eskian M, Lococo F, Yi SK, Iwano S, Meysamie A, Lapa C, Gea J, Viglianti BL, Jacobsson H, Pitman AG, Tatcı E, Khorasanizadeh M, Sancho-Muñoz A, Peters M, John J, Boktor RR, Bybel B, Alavi A, Rezaei N, Keramida G, Caobelli F, Schildt J, Barwick TD, Mazurek T. Effect of blood glucose level on standardized uptake value (SUV) in ^{18}F-FDG PET-scan: a systematic review and meta-analysis of 20,807 individual SUV measurements. *Eur J Nucl Med Mol Imaging* 2019;**46**:224–237.
54. Papadopoulos V, Baraldi M, Guilarte TR, Knudsen TB, Lacapère JJ, Lindemann P, Norenberg MD, Nutt D, Weizman A, Zhang MR, Gavish M. Translocator protein (18 kDa): new nomenclature for the peripheral-type benzodiazepine receptor based on its structure and molecular function. *Trends Pharmacol Sci* 2006;**27**: 402–409.
55. Selvaraj V, Stocco DM. The changing landscape in translocator protein (TSPO) function. *Trends Endocrinol Metab* 2015;**26**:341–348.
56. Fujimura Y, Hwang PM, Trout H, Kozloff L, Imaizumi M, Innis RB, Fujita M. Increased peripheral benzodiazepine receptors in arterial plaque of patients with atherosclerosis: an autoradiographic study with [^{3}H]PK 11195. *Atherosclerosis* 2008; **201**:108–111.
57. Bird JLE, Izquierdo-Garcia D, Davies JR, Rudd JHF, Probst KC, Figg N, Clark JC, Weissberg PL, Davenport AP, Warburton EA. Evaluation of translocator protein quantification as a tool for characterising macrophage burden in human carotid atherosclerosis. *Atherosclerosis* 2010;**210**:388–391.
58. Wilms H, Claasen J, Röhl C, Sievers J, Deuschl G, Lucius R. Involvement of benzodiazepine receptors in neuroinflammatory and neurodegenerative diseases: evidence from activated microglial cells *in vitro*. *Neurobiol Dis* 2003;**14**:417–424.
59. Cosenza-Nashat M, Zhao ML, Suh HS, Morgan J, Natividad R, Morgello S, Lee SC. Expression of the translocator protein of 18 kDa by microglia, macrophages and astrocytes based on immunohistochemical localization in abnormal human brain. *Neuropathol Appl Neurobiol* 2009;**35**:306–328.
60. Pike VW, Halldin C, Crouzel C, Barré L, Nutt DJ, Osman S, Shah F, Turton DR, Waters SL. Radioligands for PET studies of central benzodiazepine receptors and PK (peripheral benzodiazepine) binding sites-current status. *Nucl Med Biol* 1993;**20**: 503–525.
61. Laitinen I, Marjamäki P, Någren K, Laine VJO, Wilson I, Leppänen P, Ylä-Herttuala S, Roivainen A, Knuuti J. Uptake of inflammatory cell marker [^{11}C]PK11195 into mouse atherosclerotic plaques. *Eur J Nucl Med Mol Imaging* 2009;**36**:73–80.
62. Guo Q, Owen DR, Rabiner EA, Turkheimer FE, Gunn RN. Identifying improved TSPO PET imaging probes through biomathematics: the impact of multiple TSPO binding sites *in vivo*. *Neuroimage* 2012;**60**:902–910.
63. Cuhlmann S, Gsell W, Heiden KVD, Habib J, Tremoleda JL, Khalil M, Turkheimer F, Meens MJ, Kwak BR, Bird J, Davenport AP, Clark J, Haskard D, Krams R, Jones H, Evans PC. *In vivo* mapping of vascular inflammation using the translocator protein tracer ^{18}F-FEDAA1106. *Mol Imaging* 2014;**13**. doi:10.2310/7290.2014.00014.
64. Hellberg S, Silvola JMU, Kiugel M, Liljenbäck H, Savisto N, Li X-G, Thiele A, Lehmann L, Heinrich T, Vollmer S, Hakovirta H, Laine VJO, Ylä-Herttuala S, Knuuti J, Roivainen A, Saraste A. 18-kDa translocator protein ligand ^{18}F-FEMPA: biodistribution and uptake into atherosclerotic plaques in mice. *J Nucl Cardiol* 2017;**24**: 862–871.
65. Hellberg S, Liljenbäck H, Eskola O, Morisson-Iveson V, Morrison M, Trigg W, Saukko P, Ylä-Herttuala S, Knuuti J, Saraste A, Roivainen A. Positron emission tomography imaging of macrophages in atherosclerosis with ^{18}F-GE-180, a radiotracer for translocator protein (TSPO). *Contrast Media Mol Imaging* 2018;**2018**:9186902.
66. Gaemperli O, Shalhoub J, Owen DRJ, Lamare F, Johansson S, Fouladi N, Davies AH, Rimoldi OE, Camici PG. Imaging intraplaque inflammation in carotid atherosclerosis with ^{11}C-PK11195 positron emission tomography/computed tomography. *Eur Heart J* 2012;**33**:1902–1910.
67. Janssen B, Vugts DJ, Funke U, Molenaar GT, Kruijer PS, Berckel B V, Lammertsma AA, Windhorst AD. Imaging of neuroinflammation in Alzheimer's disease, multiple sclerosis and stroke: recent developments in positron emission tomography. *Biochim Biophys Acta* 2016;**1862**:425–441.
68. Owen DR, Yeo AJ, Gunn RN, Song K, Wadsworth G, Lewis A, Rhodes C, Pulford DJ, Bennacef I, Parker CA, StJean PL, Cardon LR, Mooser VE, Matthews PM, Rabiner EA, Rubio JP. An 18-kDa translocator protein (TSPO) polymorphism explains differences in binding affinity of the PET radioligand PBR28. *J Cereb Blood Flow Metab* 2012;**32**:1–5.
69. Owen DRJ, Gunn RN, Rabiner EA, Bennacef I, Fujita M, Kreisl WC, Innis RB, Pike VW, Reynolds R, Matthews PM, Parker CA. Mixed-affinity binding in humans with 18-kDa translocator protein ligands. *J Nucl Med* 2011;**52**:24–32.
70. Ikawa M, Lohith TG, Shrestha S, Telu S, Zoghbi SS, Castellano S, Taliani S, Settimo FD, Fujita M, Pike VW, Innis RB. ^{11}C-ER176, a radioligand for 18-kDa translocator protein, has adequate sensitivity to robustly image all three affinity genotypes in human brain. *J Nucl Med* 2017;**58**:320–325.
71. O'Brien KD, Kuusisto J, Reichenbach DD, Ferguson M, Giachelli C, Alpers CE, Otto CM. Osteopontin is expressed in human aortic valvular lesions. *Circulation* 1995;**92**: 2163–2168.
72. Jenkins WSA, Vesey AT, Shah ASV, Pawade TA, Chin CWL, White AC, Fletcher A, Cartlidge TRG, Mitchell AJ, Pringle MAH, Brown OS, Pessotto R, McKillop G, Beek EV, Boon NA, Rudd JHF, Newby DE, Dweck MR. Valvular ^{18}F-fluoride and ^{18}F-fluorodeoxyglucose uptake predict disease progression and clinical outcome in patients with aortic stenosis. *J Am Coll Cardiol* 2015;**66**:1200–1201.
73. Irkle A, Vesey AT, Lewis DY, Skepper JN, Bird JLE, Dweck MR, Joshi FR, Gallagher FA, Warburton EA, Bennett MR, Brindle KM, Newby DE, Rudd JH, Davenport AP. Identifying active vascular microcalcification by (18)F-sodium fluoride positron emission tomography. *Nat Commun* 2015;**6**:7495.
74. Budoff MJ, Gul KM. Expert review on coronary calcium. *Vasc Health Risk Manag* 2008;**4**:315–324.
75. McEvoy JW, Blaha MJ, DeFilippis AP, Budoff MJ, Nasir K, Blumenthal RS, Jones SR. Coronary artery calcium progression: an important clinical measurement? *J Am Coll Cardiol* 2010;**56**:1613–1622.

76. Czernin J, Satyamurthy N, Schiepers C. Molecular mechanisms of bone ^{18}F-NaF deposition. *J Nucl Med* 2010;**51**:1826–1829.
77. Creager MD, Hohl T, Hutcheson JD, Moss AJ, Schlotter F, Blaser MC, Park M-A, Lee LH, Singh SA, Alcaide-Corral CJ, Tavares AAS, Newby DE, Kijewski MF, Aikawa M, M Di C, Dweck MR, Aikawa E. ^{18}F-fluoride signal amplification identifies microcalcifications associated with atherosclerotic plaque instability in positron emission tomography/computed tomography images. *Circ Cardiovasc Imaging* 2019;**12**: e007835.
78. Vesey AT, Jenkins WSA, Irkle A, Moss A, Sng G, Forsythe RO, Clark T, Roberts G, Fletcher A, Lucatelli C, Rudd JHF, Davenport AP, Mills NL, Al-Shahi Salman R, Dennis M, Whiteley WN, Beek EV, Dweck MR, Newby DE. ^{18}F-fluoride and ^{18}F-fluorodeoxyglucose positron emission tomography after transient ischemic attack or minor ischemic stroke: case-control study. *Circ Cardiovasc Imaging* 2017;**10**:1–10.
79. Marchesseau S, Seneviratna A, Sjöholm AT, Qin DL, Ho JXM, Hausenloy DJ, Townsend DW, Richards AM, Totman JJ, Chan MYY. Hybrid PET/CT and PET/MRI imaging of vulnerable coronary plaque and myocardial scar tissue in acute myocardial infarction. *J Nucl Cardiol* 2018;**25**:2001–2011.
80. Kwiecinski J, Dey D, Cadet S, Lee S-E, Otaki Y, Huynh PT, Doris MK, Eisenberg E, Yun M, Jansen MA, Williams MC, Tamarappoo BK, Friedman JD, Dweck MR, Newby DE, Chang H-J, Slomka PJ, Berman DS. Peri-coronary adipose tissue density is associated with ^{18}F-sodium fluoride coronary uptake in stable patients with high-risk plaques. *JACC Cardiovasc Imaging* 2019;doi:10.1016/j.jcmg.2018.11.032.
81. Derlin T, Richter U, Bannas P, Begemann P, Buchert R, Mester J, Klutmann S. Feasibility of ^{18}F-sodium fluoride PET/CT for imaging of atherosclerotic plaque. *J Nucl Med* 2010;**51**:862–865.
82. Derlin T, Wisotzki C, Richter U, Apostolova I, Bannas P, Weber C, Mester J, Klutmann S. *In vivo* imaging of mineral deposition in carotid plaque using ^{18}F-sodium fluoride PET/CT: correlation with atherogenic risk factors. *J Nucl Med* 2011;**52**: 362–368.
83. Dweck MR, Chow MWL, Joshi NV, Williams MC, Jones C, Fletcher AM, Richardson H, White A, McKillop G, Beek EV, Boon NA, Rudd JHF, Newby DE. Coronary arterial ^{18}F-sodium fluoride uptake: a novel marker of plaque biology. *J Am Coll Cardiol* 2012;**59**:1539–1548.
84. Joshi NV, Vesey AT, Williams MC, Shah AS, Calvert PA, Craighead FH, Yeoh SE, Wallace W, Salter D, Fletcher AM, van Beek EJ, Flapan AD, Uren NG, Behan MW, Cruden NL, Mills NL, Fox KA, Rudd JH, Dweck MR, Newby DE. ^{18}F-fluoride positron emission tomography for identification of ruptured and high-risk coronary atherosclerotic plaques: a prospective clinical trial. *Lancet* 2014;**383**:705–713.
85. McKenney-Drake ML, Territo PR, Salavati A, Houshmand S, Persohn S, Liang Y, Alloosh M, Moe SM, Weaver CM, Alavi A, Sturek M. ^{18}F-NaF PET Imaging of Early Coronary Artery Calcification. *JACC Cardiovasc Imaging* 2016;**9**:627–8.
86. van der Vorst EP, Döring Y, Weber C. Chemokines and their receptors in atherosclerosis. *J Mol Med* 2015;**93**:963–971.
87. Akhtar S, Gremse F, Kiessling F, Weber C, Schober A. CXCL12 promotes the stabilization of atherosclerotic lesions mediated by smooth muscle progenitor cells in Apoe-deficient mice. *Arterioscler Thromb Vasc Biol* 2013;**33**:679–686.
88. Yao L, Heuser-Baker J, Herlea-Pana O, Iida R, Wang Q, Zou M-H, Barlic-Dicen J. Bone marrow endothelial progenitors augment atherosclerotic plaque regression in a mouse model of plasma lipid lowering. *Stem Cells* 2012;**30**:2720–2731.
89. Hyafil F, Pelisek J, Laitinen I, Schottelius M, Mohring M, Döring Y, van der Vorst EP, Kallmayer M, Steiger K, Poschenrieder A, Notni J, Fischer J, Baumgartner C, Rischpler C, Nekolla SG, Weber C, Eckstein HH, Wester HJ, Schwaiger M. Imaging the cytokine receptor CXCR4 in atherosclerotic plaques with the radiotracer ^{68}Ga-pentixafor for PET. *J Nucl Med* 2017;**58**:499–506.
90. Weiberg D, Thackeray JT, Daum G, Sohns JM, Kropf S, Wester H-J, Ross TL, Bengel FM, Derlin T. Clinical molecular imaging of chemokine receptor CXCR4 expression in atherosclerotic plaque using ^{68}Ga-pentixafor PET: correlation with cardiovascular risk factors and calcified plaque burden. *J Nucl Med* 2017;**59**:266–272.
91. Li X, Heber D, Leike T, Beitzke D, Lu X, Zhang X, Wei Y, Mitterhauser M, Wadsak W, Kropf S, Wester HJ, Loewe C, Hacker M, Haug AR. [^{68}Ga]Pentixafor-PET/MRI for the detection of Chemokine receptor 4 expression in atherosclerotic plaques. *Eur J Nucl Med Mol Imaging* 2018;**45**:558–566.
92. Derlin T, Sedding DG, Dutzmann J, Haghikia A, König T, Napp LC, Schütze C, Owsianski-Hille N, Wester H-J, Kropf S, Thackeray JT, Bankstahl JP, Geworski L, Ross TL, Bauersachs J, Bengel FM. Imaging of chemokine receptor CXCR4 expression in culprit and nonculprit coronary atherosclerotic plaque using motion-corrected [^{68}Ga]pentixafor PET/CT. *Eur J Nucl Med Mol Imaging* 2018;**45**: 1934–1944.
93. Krantic S. Peptides as regulators of the immune system: emphasis on somatostatin. *Peptides* 2000;**21**:1941–64.
94. Dalm V, van Hagen PM, van Koetsveld PM, Achilefu S, Houtsmuller AB, Pols DH, van der Lely AJ, Lamberts SW, Hofland LJ. Expression of somatostatin, cortistatin, and somatostatin receptors in human monocytes, macrophages, and dendritic cells. *Am J Physiol Endocrinol Metab* 2003;**285**:E344–E353.
95. Froidevaux S, Eberle AN, Christe M, Sumanovski L, Heppeler A, Schmitt JS, Eisenwiener K, Beglinger C, Mäcke HR. Neuroendocrine tumor targeting: study of novel gallium-labeled somatostatin radiopeptides in a rat pancreatic tumor model. *Int J Cancer* 2002;**98**:930–937.
96. Li X, Bauer W, Kreissl MC, Weirather J, Bauer E, Israel I, Richter D, Riehl G, Buck A, Samnick S. Specific somatostatin receptor II expression in arterial plaque: ^{68}Ga-DOTATATE autoradiographic, immunohistochemical and flow cytometric studies in apoE-deficient mice. *Atherosclerosis* 2013;**230**:33–39.
97. Rinne P, Hellberg S, Kiugel M, Virta J, Li X-G, Käkelä M, Helariutta K, Luoto P, Liljenbäck H, Hakovirta H, Gardberg M, Airaksinen AJ, Knuuti J, Saraste A, Roivainen A. Comparison of somatostatin receptor 2-targeting PET tracers in the detection of mouse atherosclerotic plaques. *Mol Imaging Biol* 2016;**18**:99–108.
98. Rominger A, Saam T, Vogl E, Ubleis C, Fougere C. L, Forster S, Haug A, Cumming P, Reiser MF, Nikolaou K, Bartenstein P, Hacker M. *In vivo* imaging of macrophage activity in the coronary arteries using ^{68}Ga-DOTATATE PET/CT: correlation with coronary calcium burden and risk factors. *J Nucl Med* 2010;**51**:193–197.
99. Wan MYS, Endozo R, Michopoulou S, Shortman R, Rodriguez-Justo M, Menezes L, Yusuf S, Richards T, Wild D, Waser B, Reubi JC, Groves A. PET/CT imaging of unstable carotid plaque with ^{68}Ga-labeled somatostatin receptor ligand. *J Nucl Med* 2017;**58**:774–780.
100. Tarkin JM, Joshi FR, Evans NR, Chowdhury MM, Figg NL, Shah AV, Starks LT, Martin-Garrido A, Manavaki R, Yu E, Kuc RE, Grassi L, Kreuzhuber R, Kostadima MA, Frontini M, Kirkpatrick PJ, Coughlin PA, Gopalan D, Fryer TD, Buscombe JR, Groves AM, Ouwehand WH, Bennett MR, Warburton EA, Davenport AP, Rudd J. Detection of atherosclerotic inflammation by ^{68}Ga-DOTATATE PET compared to [^{18}F]FDG PET imaging. *J Am Coll Cardiol* 2017;**69**:1774–1791.
101. Xia W, Hilgenbrink AR, Matteson EL, Lockwood MB, Cheng JX, Low PS. A functional folate receptor is induced during macrophage activation and can be used to target drugs to activated macrophages. *Blood* 2009;**113**:438–446.
102. Paulos CM, Varghese B, Widmer WR, Breur GJ, Vlashi E, Low PS. Folate-targeted immunotherapy effectively treats established adjuvant and collagen-induced arthritis. *Arthritis Res Ther* 2006;**8**:R77.
103. Ayala-Lopez W, Xia W, Varghese B, Low PS. Imaging of atherosclerosis in apolipoprotein E knockout mice: targeting of a folate-conjugated radiopharmaceutical to activated macrophages. *J Nucl Med* 2010;**51**:768–774.
104. Jager NA, Westra J, Golestani R, Dam G. V, Low PS, Tio RA, Slart R, Boersma HH, Bijl M, Zeebregts CJ. Folate receptor-imaging using 99mTc-folate to explore distribution of polarized macrophage populations in human atherosclerotic plaque. *J Nucl Med* 2014;**55**:1945–1951.
105. Silvola JMU, Li XG, Virta J, Marjamäki P, Liljenbäck H, Hytönen JP, Tarkia M, Saunavaara V, Hurme S, Palani S, Hakovirta H, Ylä-Herttuala S, Saukko P, Chen Q, Low PS, Knuuti J, Saraste A, Roivainen A. Aluminum fluoride-18 labeled folate enables *in vivo* detection of atherosclerotic plaque inflammation by positron emission tomography. *Sci Rep* 2018;**8**:1–15.
106. Cuccurullo C, Fazia M, Mezzetti A, Cipollone F. COX-2 expression in atherosclerosis: the good, the bad or the ugly? *Curr Med Chem* 2007;**14**:1595–1605.
107. Thackeray J, Ross TL, Bankstahl J, Wester H, Bengel F. Targeting cardiovascular inflammation for imaging: comparison of the uptake of multiple tracers in leukocyte subpopulations. *J Nucl Med* 2017;**58**:302.
108. Thackeray JT, Hupe HC, Wang Y, Bankstahl JP, Berding G, Ross TL, Bauersachs J, Wollert KC, Bengel FM. Myocardial inflammation predicts remodeling and neuroinflammation after myocardial infarction. *J Am Coll Cardiol* 2018;**71**:263–275.
109. Liu L, Shi G-P. CD31: beyond a marker for endothelial cells. *Cardiovasc Res* 2012;**94**: 3–5.
110. Gurevich DB, Severn CE, Twomey C, Greenhough A, Cash J, Toye AM, Mellor H, Martin P. Live imaging of wound angiogenesis reveals macrophage orchestrated vessel sprouting and regression. *EMBO J* 2018;**37**:e97786.
111. Brooks P, Clark R, Cheresh D. a. Requirement of vascular integrin alpha(V)beta(3) for angiogenesis. *Science* 1994;**264**:569–571.
112. Hoshiga M, Alpers CE, Smith LL, Giachelli CM, Schwartz SM. αvβ3 integrin expression in normal and atherosclerotic artery. *Circ Res* 1995;**77**:1129–1135.
113. Antonov AS, Kolodgie FD, Munn DH, Gerrity RG. Regulation of macrophage foam cell formation by αVβ3 integrin: potential role in human atherosclerosis. *Am J Pathol* 2004;**165**:247–258.
114. Laitinen I, Saraste A, Weidl E, Poethko T, Weber AW, Nekolla SG, LeppäNen P, Ylä-Herttuala S, HöLzlwimmer G, Walch A, Esposito I, Wester H-J, Knuuti J, Schwaiger M. Evaluation of αvβ3integrin-targeted positron emission tomography tracer ^{18}F-galacto-RGD for imaging of vascular inflammation in atherosclerotic mice. *Circ Cardiovasc Imaging* 2009;**2**:331–338.
115. Beer AJ, Pelisek J, Heider P, Saraste A, Reeps C, Metz S, Seidl S, Kessler H, Wester HJ, Eckstein HH, Schwaiger M. PET/CT imaging of integrin αvβ3 expression in human carotid atherosclerosis. *JACC Cardiovasc Imaging* 2014;**7**:178–187.
116. Battle MR, Goggi JL, Allen L, Barnett J, Morrison MS. Monitoring tumor response to antiangiogenic sunitinib therapy with ^{18}F-fluciclatide, an ^{18}F-labeled a. *J Nucl Med* 2011;**52**:424–430.
117. Joshi NV, Toor I, Shah AS, Carruthers K, Vesey AT, Alam SR, Sills A, Hoo TY, Melville AJ, Langlands SP, Jenkins WS, Uren NG, Mills NL, Fletcher AM, van Beek EJ, Rudd JH, Fox KA, Dweck MR, Newby DE. Systemic atherosclerotic inflammation following acute myocardial infarction: myocardial infarction begets myocardial infarction. *J Am Heart Assoc* 2015;**4**:e001956.
118. Chen DL, Schiebler ML, Goo JM, van Beek EJR. PET imaging approaches for inflammatory lung diseases: current concepts and future directions. *Eur J Radiol* 2017;**86**: 371–376.

119. Albuquerque EX, Alkondon M, Pereira EF, Castro NG, Schrattenholz A, Barbosa CT, Bonfante-Cabarcas R, Aracava Y, Eisenberg HM, Maelicke A. Properties of neuronal nicotinic acetylcholine receptors: pharmacological characterization and modulation of synaptic function. *J Pharmacol Exp Ther* 1997;**280**:1117–1136.
120. Conti-Fine BM, Navaneetham D, Lei S, Maus ADJ. Neuronal nicotinic receptors in non-neuronal cells: new mediators of tobacco toxicity? *Eur J Pharmacol* 2000;**393**: 279–294.
121. Heeschen C, Weis M, Aicher A, Dimmeler S, Cooke JP. A novel angiogenic pathway mediated by non-neuronal nicotinic acetylcholine receptors. *J Clin Invest* 2002;**110**: 527–536.
122. Lee RH, Vazquez G. Evidence for a prosurvival role of alpha-7 nicotinic acetylcholine receptor in alternatively (M2)-activated macrophages. *Physiol Rep* 2013;**1**:e00189.
123. Kanaoka Y, Koga M, Sugiyama K, Ohishi K, Kataoka Y, Yamauchi A. Varenicline enhances oxidized LDL uptake by increasing expression of LOX-1 and CD36 scavenger receptors through α7 nAChR in macrophages. *Toxicology* 2017;**380**:62–71.
124. Koga M, Kanaoka Y, Ohkido Y, Kubo N, Ohishi K, Sugiyama K, Yamauchi A, Kataoka Y. Varenicline aggravates plaque formation through α7 nicotinic acetylcholine receptors in ApoE KO mice. *Biochem Biophys Res Commun* 2014;**455**:194–197.
125. Kooijman S, Meurs I, van der Stoep M, Habets KL, Lammers B, Berbée JF, Havekes LM, van Eck M, Romijn JA, Korporaal SJ, Rensen PC. Hematopoietic α7 nicotinic acetylcholine receptor deficiency increases inflammation and platelet activation status, but does not aggravate atherosclerosis. *J Thromb Haemost* 2015;**13**:126–135.
126. Boswijk E, Bauwens M, Mottaghy FM, Wildberger JE, Bucerius J. Potential of α7 nicotinic acetylcholine receptor PET imaging in atherosclerosis. *Methods* 2017;**130**:90–104.
127. Wong DF, Kuwabara H, Pomper M, Holt DP, Brasic JR, George N, Frolov B, Willis W, Gao Y, Valentine H, Nandi A, Gapasin L, Dannals RF, Horti AG. Human brain imaging of α7 nAChR with [^{18}F]ASEM: a new PET radiotracer for neuropsychiatry and determination of drug occupancy. *Mol Imaging Biol* 2014;**16**:730–738.
128. Hillmer AT, Li S, Zheng M-Q, Scheunemann M, Lin S, Nabulsi N, Holden D, Pracitto R, Labaree D, Ropchan J, Teodoro R, Deuther-Conrad W, Esterlis I, Cosgrove KP, Brust P, Carson RE, Huang Y. PET imaging of α7 nicotinic acetylcholine receptors: a comparative study of [^{18}F]ASEM and [^{18}F]DBT-10 in nonhuman primates, and further evaluation of [^{18}F]ASEM in humans. *Eur J Nucl Med Mol Imaging* 2017;**44**:1042–1050.
129. Magnussen JH, Ettrup A, Donat CK, Peters D, Pedersen MHF, Knudsen GM, Mikkelsen JD. Radiosynthesis and *in vitro* validation of ^{3}H-NS14492 as a novel high affinity alpha7 nicotinic receptor radioligand. *Eur J Pharmacol* 2015;**762**:35–41.
130. Rötering S, Scheunemann M, Fischer S, Hiller A, Peters D, Deuther-Conrad W, Brust P. Radiosynthesis and first evaluation in mice of [^{18}F]NS14490 for molecular imaging of α7 nicotinic acetylcholine receptors. *Bioorg Med Chem* 2013;**21**:2635–2642.
131. Rötering S, Deuther-Conrad W, Cumming P, Donat CK, Scheunemann M, Fischer S, Xiong G, Steinbach J, Peters D, Sabri O, Bucerius J, Brust P. Imaging of α7 nicotinic acetylcholine receptors in brain and cerebral vasculature of juvenile pigs with [^{18}F]NS14490. *EJNMMI Res* 2014;**4**:43.
132. Aukrust P, Halvorsen B, Ueland T, Michelsen AE, Skjelland M, Gullestad L, Yndestad A, Otterdal K. Activated platelets and atherosclerosis. *Expert Rev Cardiovasc Ther* 2010;**8**:1297–1307.
133. Ikuta T, Naruko T, Ikura Y, Ohsawa M, Fukushima H, Shirai N, Itoh A, Haze K, Ehara S, Sasaki Y, Shibata T, Suehiro S, Ueda M. Immunolocalization of platelet glycoprotein IIb/IIIa and P-selectin, and neutrophil-platelet interaction in human coronary unstable plaques. *Int J Mol Med* 2005;**15**:573–577.
134. Shen S, Guo S, Wang H, Li M, Liu Y, Bin J, Hou F, Wang J, Liao Y. Detection of high-risk atherosclerotic plaques with ultrasound molecular imaging of glycoprotein IIb/IIIa receptor on activated platelets. *Theranostics* 2015;**5**:418–430.
135. Chae SY, Kwon TW, Jin S, Kwon SU, Sung C, Oh SJ, Lee SJ, Oh JS, Han Y, Cho YP, Lee N, Kim JY, Koglin N, Berndt M, Stephens AW, Moon DH. A phase 1, first-in-human study of ^{18}F-GP1 positron emission tomography for imaging acute arterial thrombosis. *EJNMMI Res* 2019;**9**:3.
136. Bitto A, De Caridi G, Polito F, Calò M, Irrera N, Altavilla D, Spinelli F, Squadrito F. Evidence for markers of hypoxia and apoptosis in explanted human carotid atherosclerotic plaques. *J Vasc Surg* 2010;**52**:1015–1021.
137. Dubois LJ, Lieuwes NG, Janssen MH, Peeters WJ, Windhorst AD, Walsh JC, Kolb HC, Ollers MC, Bussink J, van Dongen GA, van der Kogel A, Lambin P. Preclinical evaluation and validation of [^{18}F]HX4, a promising hypoxia marker for PET imaging. *Proc Natl Acad Sci USA* 2011;**108**:14620–14625.
138. van der Valk FM, Sluimer JC, Vöö SA, Verberne HJ, Nederveen AJ, Windhorst AD, Stroes ES, Lambin P, Daemen MJ. *In vivo* imaging of hypoxia in atherosclerotic plaques in humans. *JACC Cardiovasc Imaging* 2015;**8**:1340–1341.
139. Cohen A, Shirvan A, Levin G, Grimberg H, Reshef A, Ziv I. From the Gla domain to a novel small-molecule detector of apoptosis. *Cell Res* 2009;**19**:625–637.
140. Hyafil F, Tran-Dinh A, Burg S, Leygnac S, Louedec L, Milliner M, Azzouna RBen, Reshef A, Ben Ami M, Meilhac O, Le Guludec D. Detection of apoptotic cells in a rabbit model with atherosclerosis-like lesions using the positron emission tomography radiotracer [^{18}F]ML-10. *Mol Imaging* 2015;**14**:433–442.
141. Derlin T, Toth Z, Papp L, Wisotzki C, Apostolova I, Habermann CR, Mester J, Klutmann S. Correlation of inflammation assessed by 18F-FDG PET, active mineral deposition assessed by ^{18}F-fluoride PET, and vascular calcification in atherosclerotic plaque: a dual-tracer PET/CT study. *J Nucl Med* 2011;**52**:1020–1027.
142. Guo J, Guo N, Lang L, Kiesewetter DO, Xie Q, Li Q, Eden HS, Niu G, Chen X. ^{18}F-Alfatide II and ^{18}F-FDG dual-tracer dynamic PET for parametric, early prediction of tumor response to therapy. *J Nucl Med* 2014;**55**:154–160.
143. Stefanadis C, Antoniou C, Tsiachris D, Pietri P. Coronary atherosclerotic vulnerable plaque: current perspectives. *J Am Heart Assoc* 2017;**6**:e005543.
144. Adamson PD, Dweck MR, Newby DE. The vulnerable atherosclerotic plaque: *in vivo* identification and potential therapeutic avenues. *Heart* 2015;**101**:1755–1766.
145. Dweck MR, Aikawa E, Newby DE, Tarkin JM, Rudd JHF, Narula J, Fayad ZA. Noninvasive molecular imaging of disease activity in atherosclerosis. *Circ Res* 2016; **119**:330–340.